Hierarchical Modelling of Entangled Polymer Melts: Structure and Rheology

H.-P. Hsu, G. Zhang, T. Stuehn, K. Ch. Daoulas, K. Kremer

published in

NIC Symposium 2018
K. Binder, M. Müller, A. Trautmann (Editors)

Forschungszentrum Jülich GmbH,
John von Neumann Institute for Computing (NIC),
Schriften des Forschungszentrums Jülich, NIC Series, Vol. 49,
ISBN 978-3-95806-285-6, pp. 303.
http://hdl.handle.net/2128/17544

Hierarchical Modelling of Entangled Polymer Melts: Structure and Rheology

Hsiao-Ping Hsu[1], **Guojie Zhang**[2], **Torsten Stuehn**[1], **Kostas Ch. Daoulas**[1], **and Kurt Kremer**[1]

[1] Max Planck Institute for Polymer Research, Ackermannweg 10, 55128 Mainz, Germany
E-mail: {hsu, stuehn, daoulas, kremer}@mpip-mainz.mpg.de

[2] Institute for Theoretical Physics, Georg-August University, 37077 Göttingen, Germany
E-mail: guojie.zhang@theorie.physik.uni-goettingen.de

We describe the extension of a novel hierarchical backmapping strategy to equilibrating high-molecular-weight homopolymer melts described with chemistry-specific microscopic models. The method has been initially developed in the framework of highly entangled melts, described through generic microscopic (bead-spring) models. The systems are first efficiently equilibrated on the mesoscopic level, based on a model describing polymers as chains of soft spheres. Each sphere represents a large number of microscopic repeat units. After the mesoscopic configuration is generated, microscopic details are reinserted through Molecular Dynamics simulations. Here we demonstrate that the method can be indeed implemented to generate equilibrated configurations of actual molten polymers, considering the case of polystyrene. We illustrate how the backmapping strategy facilitates fundamental computational studies in polymer physics, focusing on two questions from the area of polymer dynamics and rheology. The highly-entangled samples described with a generic microscopic model are first employed to verify basic predictions of tube theories at equilibrium. Subsequently we address the intriguing question of how topological constraints evolve during relaxation after strong deformation.

1 Introduction

In polymers, relationships between structure, processing, and properties are often driven by mechanisms involving a broad spectrum of length and time scales[1–4]. Dynamics and consequently rheology of polymer melts are typical examples, where one can distinguish[5] the regimes of non-entangled and entangled chains. The non-entangled regime arises for short chains and can be understood within the Rouse theory. In this theory the polymer-chain dynamics is seen as a three-dimensional Brownian motion of N monomers linked by bonds. The diffusion coefficient of the chains follows from the Einstein relationship $D = kT/\zeta N$, where ζ is the friction coefficient of a single monomer and kT is the thermal energy. The entangled regime occurs when polymers are sufficiently long so that the non-crossability of the chains due to *microscopic* excluded volume leads to temporal topological constraints that determine dynamic properties. The average number of monomers between two consecutive topological constraints is given by the entanglement length, N_{e}. One of the cornerstones of modern polymer physics is the insight[6,7] that entanglements force a test chain to "reptate" along the contour of an effective tube[5–13]. The tube is transient as its parts are continuously renewed[5] through the motion of chain-ends. The reptation along the tube contour itself presents a one-dimensional diffusion following Rouse dynamics. However the actual trajectory of a chain in the three-dimensional space is determined by the arrangement of the tube, presenting a randomly coiled thread. The net effect is that the diffusion coefficient of entangled chains scales with the number of monomers

as $D \sim kTN_{\rm e}/\zeta N^2$. This scaling illustrates the protracted dynamics of entangled macromolecules and explains why studying polymer rheology with computer simulations is so challenging.

Computational studies are an important tool for understanding nonlinear polymer rheology. This regime presents great interest for fundamental science and industry but is only partially understood. Refined tube theories[5,8,13] accounting for tube contour-length fluctuations[9,10] and constraint-release[9,11,12] can capture important features in experimental observations (e.g. birefringence and neutron scattering patters in contraction flow[14]) Nevertheless, the mechanisms of polymer relaxation in the non-linear viscoelastic regime (for example, pathway of chain retraction) are still under debate[15–18].

For conceptual studies of polymer dynamics and rheology generic bead-spring-type models are preferable. These models have[19] realistic microscopic features (such as hard excluded volume, strong covalent bonds, and high density) but are more efficient computationally, comparing to chemistry-specific descriptions. Some of the reasons are: a) simpler potentials and b) accessing highly entangled regimes with shorter chains by decreasing $N_{\rm e}$ through generic manipulation[20] of molecular stiffness. Using generic microscopic models, one can perform computational analogs of actual rheological experiments, such as step elongation, step and startup shear. These simulations must be performed with truly dynamical, e.g. Molecular Dynamics (MD) methods and, therefore, are costly. However, with supercomputers and highly optimised software such studies are becoming feasible. The polymer sample used to initiate the rheological simulations must be perfectly equilibrated at all scales. Generating such samples is challenging and requires special techniques circumventing the prohibitively large relaxation times in MD.

Large samples of highly entangled polymer melts can be equilibrated through divide-and-conquer hierarchical strategies[4]. These approaches consider the polymer sample on several levels of resolution, covering the range from mesoscopic to atomistic scales. Each level is described by an appropriate model. The sample is first equilibrated with coarser resolution and one proceeds reinserting the degrees of freedom of the next level. This reinsertion requires only local computations and is therefore very efficient. Descending the levels of hierarchy one finally generates a fully equilibrated microscopically-resolved sample. Recently such a hierarchical strategy based on coarse-grained representations of polymers as strings of soft spheres (blobs) has been developed[21,22]. Stepwise fine-graining of configurations equilibrated at low resolution is employed, until reaching a blob-based representation with sufficiently high resolution to allow reinsertion of microscopic details. The method has been used to generate a library of samples[21,22] of equilibrated melts of unprecedented size and chain-length, i.e. number of chains in the sample $\sim 10^3$ and polymerisation degree $\sim 10^2\ N_e$. Currently this library of samples is available for rheological studies. The success of the new equilibration method in generic microscopic models motivates further developments for handling chemically-specific descriptions, since this will enable computational studies of rheology of actual polymeric materials.

In the first part of this work, we demonstrate that hierarchical strategies engaging mesoscopic blob-based representations can be indeed implemented to equilibrate melts described with microscopic chemistry-specific models. Polystyrene (PS) melts (a basic commodity polymer) are considered as a test case. These systems are well suited for testing modelling techniques since PS molecules are sufficiently complex, exhibiting features such as tacticity and bulky units (benzene rings). In the second part, we will illustrate how the library of equilibrated highly-entangled melts[21,22] described with the generic microscopic model, enables fundamental studies of polymer dynamics and rheology.

2 Hierarchical Backmapping of a Chemistry-Specific Model

2.1 Microscopic and Blob-Based Models of Polystyrene

For the microscopic representation of PS we employ a moderately coarse-grained (CG) model[23], which can *quantitatively* predict properties of PS melts[24]. Algorithms for reinserting atomistic details into configurations described with this moderately coarse-grained model are already available[23]. Hence developing a hierarchical backmapping strategy for equilibrating large, highly entangled samples of PS melts described on moderately coarse-grained level, opens the way for their description with atomistic detail as well. As illustrated in Fig. 1a, the moderately CG model represents one atomistic PS monomer via two effective coarse-grained beads, A and B. Bead A corresponds to the CH_2 of a PS monomer plus the half mass of each of the two neighbouring CH groups along the chain backbone, while bead B represents the phenyl ring. The model has the significant advantage of describing tacticity of PS chains through proper bonded (angular and dihedral) potentials, without introducing side groups[23,24].

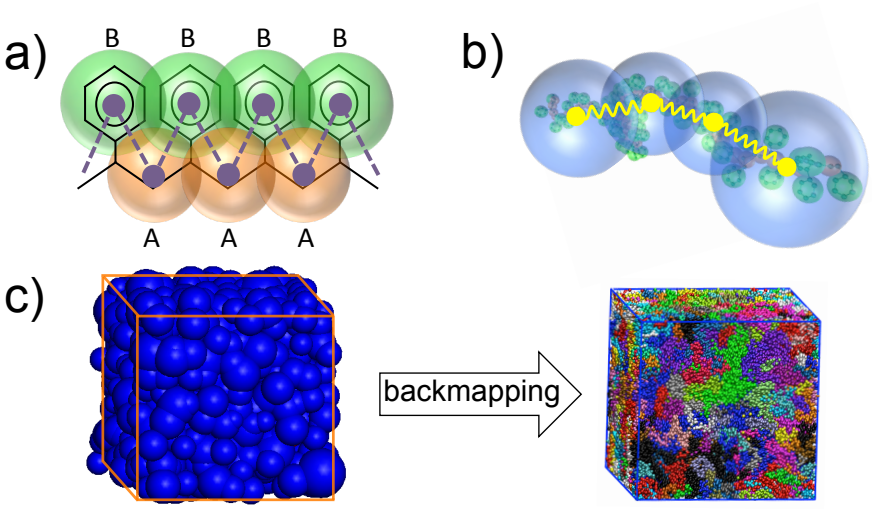

Figure 1. a) Moderately coarse-grained microscopic model of polystyrene (A and B type beads are shown in orange and green). b) Representation of a moderately CG PS molecule with a soft-sphere model (blue). For clarity each sphere is shown to represent a smaller amount of microscopic repeat units than in actual simulations. c) Left: Snapshot of a PS melt described with soft-sphere chains used to initiate backmapping. Right: Snapshot of an equilibrated PS microscopic melt (colours randomly chosen to improve visibility of different chains).

Fig. 1b illustrates the blob-based model for PS. Describing polymer melts with chains of fluctuating soft spheres has been discussed earlier[21,22,25,26]. These studies introduced the soft-sphere model for the mesoscopic representation of melts, described on microscopic level via generic bead-spring models[19]. Conceptually, connecting a soft-sphere model to the microscopic model of PS is similar. Each sphere stands for a sub-chain with N_b microscopic repeat units. The radius, σ and the location of the centre of the sphere match the

instantaneous radius of gyration and centre-of-mass (COM) of the underlying subchain. Every mesoscopic macromolecule contains N_{meso} linearly linked blobs. The connectivity of the mesoscopic chain is described[25,26] by simple harmonic bond and angular potentials, rooted[22,25] in universality concepts in polymer physics. Pairwise non-bonded interactions between blobs are given[25,26] by a Gaussian potential.

Currently there is no rigorous rule for choosing N_{b}, apart from that it must be "large enough" for the simple mesoscopic model to be valid, and small enough for the efficient reinsertion of microscopic details during backmapping (see Sec. 2.2). For PS, N_{e} is in the range of $300 - 400$ beads of the moderately CG model[24] (equivalent to $150 - 200$ atomistic monomers). Several choices of $N_{\mathrm{b}} < 200$ were considered and exploratory parameterisations of the soft-sphere model were performed. For these parameterisations we benefited from smaller samples of PS melts described with the microscopic model. These samples were equilibrated in an earlier study[23] through a variant of the configuration-assembly method[27]. Subsequently methods of systematic coarse-graining[3,4,28] are used to parameterise the mesoscopic potentials so that these descriptors are reproduced in melts of soft-sphere chains. These exploratory studies demonstrated that setting $N_{\mathrm{b}} = 120$ offers a reasonable compromise between computational efficiency of backmapping and accuracy with which the soft-sphere model describes mesoscopic conformations and liquid structure of a PS melt.

2.2 Backmapping

The left panel of Fig. 1c illustrates a configuration of a PS melt described with the soft-sphere model introduced in Sec. 2.1. The example in Fig. 1c contains $n = 200$ chains with $N_{\mathrm{meso}} = 8$ blobs (since $N_{\mathrm{b}} = 120$ these chains correspond on microscopic level to molecules with 960 repeat units). The equilibration of melts on the level of the blob-based description is very fast and is performed through an efficient Monte Carlo scheme[26]. The right panel of Fig. 1c presents a PS melt obtained by reinserting microscopic details into the mesoscopic configuration, using a procedure similar to the one developed for generic bead-spring models[21,22]. Namely, each soft-sphere polymer in the sample is replaced by a microscopic chain where only bonded interactions are activated. During this procedure the monomers of each subchain with $N_{\mathrm{b}} = 200$ monomers are subjected to external potentials. These ensure that the radius of gyration and the location of the COM of the subchain matches the radius and the COM coordinates of the corresponding blob. Once the microscopic configurations are created, non-bonded interactions between the repeat-units are introduced. The scheme recovers the microscopic hard excluded volume through a "push-off" procedure[20,27] and re-equilibration, which relaxes liquid structure and chain conformations on scales smaller or comparable to the average blob diameter. The computations required for this final re-equilibration remain feasible because of the choice $N_{\mathrm{b}} < N_{\mathrm{e}}$. This relationship warrants that the local relaxation is achieved through fast Rouse-like dynamics (time scale τ_e)[21]. For a hierarchy of sequentially fine-grained blob-based models[21], the condition $N_{\mathrm{b}} < N_{\mathrm{e}}$ applies only to the last model, where the reinsertion of the moderately CG representation is performed. Due to complexity of the PS model, MD runs corresponding to $\sim \tau_e$ are computationally still time consuming. Nevertheless they now are feasible on the JURECA supercomputer. By running the efficient ESPResSo++ code[29] on 240 CPU, samples similar to the one shown in Fig. 1c can be equilibrated within about one month (see the forthcoming paper[30]).

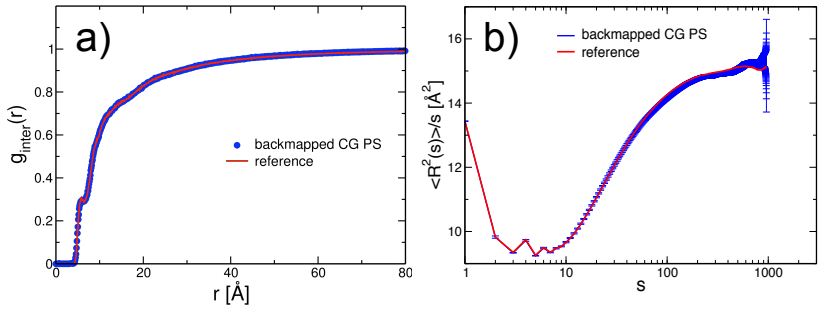

Figure 2. a) Pair-correlation functions, $g_{\mathrm{inter}}(r)$, calculated for monomers belonging to different chains in PS melts equilibrated via hierarchical backmapping (blue) and an earlier configuration-assembly procedure[23] (red). b) Internal distance plot calculated in PS melts shown in a). Blue and red colours refer to melts equilibrated via hierarchical backmapping and configuration assembly, respectively.

The excellent equilibration of backmapped PS melts was verified comparing their structural and conformational properties with data obtained from the reference PS samples[23]. As an illustration, Fig. 2a compares the pair-correlation function, $g_{\mathrm{inter}}(r)$, calculated between monomers of different chains in backmapped (blue) and reference (red) PS samples. The two curves are on top of each other, demonstrating that the backmapping reproduces correctly the long-range structure of the PS melt (correlation hole). Fig. 2b compares the internal distance plots in backmapped (blue) and reference (red) melts. The graph is obtained by presenting $\langle R^2\rangle/s$ as a function of s, where $\langle R^2\rangle$ is the mean square distance of intramolecular monomers and s is the difference of their ranking numbers along PS chain backbone. Currently the internal distance plot is considered as one of the best quantifiers[21,27,20] of system equilibration. The relative deviation of the curves in backmapped and reference samples is less than 1% verifying once more the performance of our backmapping scheme.

3 Characteristics of Fully Equilibrated and Highly Entangled Polymer Melts

Having large polymer melts containing 1000 bead-spring chains of size up to $N = 2000$ at a monomer density of $\rho = 0.85\sigma^{-3}$ in equilibrium, obtained via the methodology described above[21,20], we have the possibility to investigate not only the chain conformations but also the motion of chains on different length and time scales[32]. With an added bending potential $U(\theta) = k_\theta(1 - \cos\theta)$ controlling the stiffness of bead-spring chains[19,31], the static properties of chains characterised by $\langle R^2(s)\rangle$, and the average static structure factor $S_c(q)$ of single chains are shown in Fig. 3. We find that at $k_\theta = 1.5$, the scaling behaviour of $\langle R^2(s)\rangle$ is nearly in perfect agreement with the theoretical prediction for a freely rotating chain (FRC) which describes semiflexible chains in the absence of excluded volume effect. $S_c(q)$ presented in a Kratky-plot comparing to the scattering function $S_{\mathrm{Debye}}(q)$ for Gaussian chains also confirms the chain ideality since there is almost no deviation from

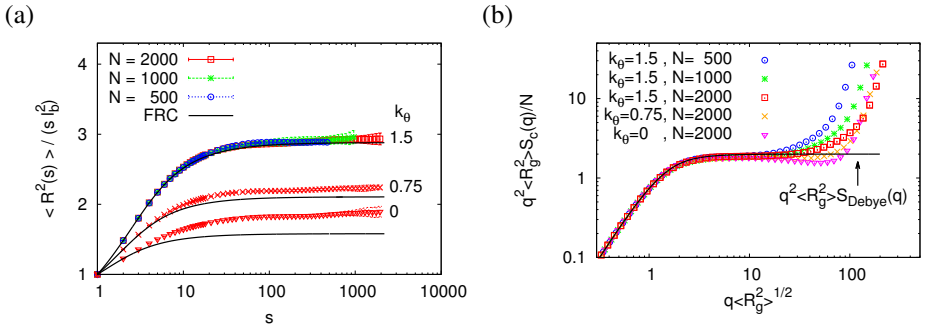

Figure 3. (a) Rescaled mean square internal distance, $\langle R^2(s)\rangle/(s\ell_b^2)$ with the bond length $\ell_b \approx 0.964\sigma$, plotted as a function of s with error bars. (b) Kratky-plot of structure factors of single chains in a melt, $S_c(q)$. Several values of k_θ and N are chosen, as indicated. The theoretical prediction for freely rotating chains (FRC) in (a), and the scattering function $S_{\rm Debye}(q)$ for Gaussian chains in (b) are also shown by solid curves for comparison[32].

Gaussian coils before the local packing effect at short length scale sets in Ref. 32.

Based on extensive molecular dynamics (MD) simulations on highly entangled polymer melts of $N = 500$ and 2000 at $k_\theta = 1.5$ (where the entanglement length $N_e \approx 28$)[20,32–34], in Fig. 4a we show results of the mean square displacement (MSD) of inner monomers and centre of mass of chains, $g_1(t)$ and $g_3(t)$, respectively, for time up to $t \approx \mathcal{O}(10^7)\tau$ (2.1×10^6 core-hrs on JURECA). The crossover scaling behaviour of MSD occurs at different time scales predicted by the Rouse model (for $N < N_e$) and reptation theory (for $N > N_e$)[5,35,36]is verified. Especially, our data of $g_1(t)$ for $N = 2000$ follow the power law $t^{1/4}$ about three decades, i.e. strongly support the reptation theory. The characteristic time $\tau_0 \approx 2.89$, the entanglement time $\tau_e \approx \tau_0 N_e^2$, and the Rouse time $\tau_{R,N} \approx \tau_0 N^2$ for $N = 500$ are determined by the intersection points of two lines from the results of $g_1(t)$. At $t = \tau_e$, $g_1(t) \sim d_T^2 \approx 2\langle R_g^2(N_e)\rangle$ leads to the tube diameter $d_T \approx 5.02\sigma$. Guided by the scaling laws, $g_1(t) \sim t^{1/2}$ for $\tau_d > t > \tau_{R,N}$ and $g_3(t) \sim t^1$ for $t > \tau_d$, our estimate of the disentanglement time $\tau_d \sim \tau_0 N^2 (N/N_e)^{1.4}$ perfectly fits the experimental result $\tau_d \propto N^{3.4}$. In the reptation regime, an analytic expression of the coherent dynamic single chain structure factor, often used for the neutron-spin-echo (NSE) measurements is given by Ref. 5, 19, 37, 38

$$\frac{S_{\rm coh}(q,t)}{S_{\rm coh}(q,0)} = \left\{\left[1-\exp\left(-\frac{q^2d^2}{36}\right)\right] f(q^2(Wt)^{1/2}) + \right. \\ \left. + \exp\left[-\frac{q^2d^2}{36}\right]\right\} \frac{8}{\pi^2} \sum_{n=1,odd}^{\infty} \frac{\exp[-tn^2/\tau_d]}{p^2} \qquad (1)$$

with $f(u) = \exp(u^2/36)\mathrm{erfc}(u/6)$, and $d = \sqrt{3}d_T$. Fitting our simulation data of $S_{\rm coh}(q,t)/S_{\rm coh}(q,0)$ to Eq. 1 as shown in Fig. 4b, it gives the tube diameter[39] $d_T \approx 5.95\sigma$ which is compatible to the estimate obtained from $g_1(t)$.

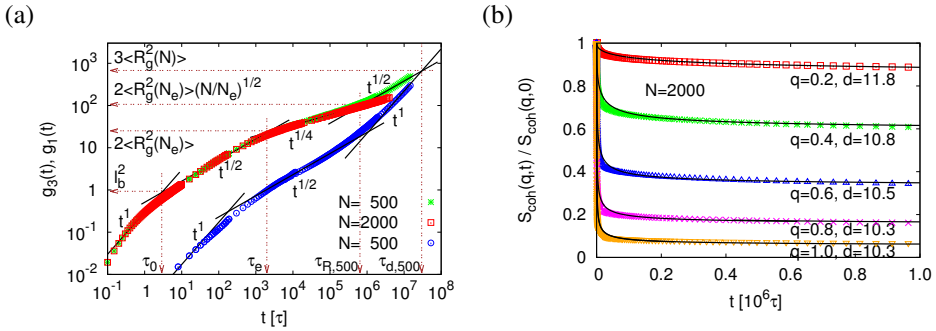

Figure 4. (a) Mean square displacement of inner monomers $g_1(t)$ and centre of mass of chains $g_3(t)$. (b) Normalised coherent dynamic structure factor, $S_{\rm coh}(q,t)/S_{\rm coh}(q,0)$, plotted versus t for five values of q, as indicated. In (a), the corresponding scaling laws at different characteristic length and time scales are marked[32]. In (b), the curves show the best fit of our data by adjusting the fitting parameter d {Eq. 1}[39].

4 Deformed Polymer Melts in Linear and Non-Linear Viscoelastic Regimes

Polymer melt dynamics are strongly affected by entanglement effects due to topological constraints between chains both in the linear and non-linear viscoelastic regime. Taking a well equilibrated polymer melt[32,39] of entanglement length $N_e \approx 28$ at $k_\theta = 1.5$ as a reference system, we apply the simplest deformation mechanism, "isochroic elongation" to stretch the system at fixed volume $V = L_x L_y L_z = L_0^3$ with a stretch ratio $\lambda = L_x/L_0$ into linear ($\lambda \approx 1.2$) and non-linear ($\lambda \approx 5.0$) viscoelastic regimes. Fig. 5 shows the stress relaxation modulus $G(t) = \sigma_{\rm norm}/(\lambda^2 - 1/\lambda)$ as a function of relaxation time t after small and large deformation with slow and fast strain rates[32,40] (8.55×10^5 core-hrs on JURECA). Here $\sigma_{\rm norm}$ is the normal stress tensor, and the strain rate $\tau_{R,N}^{-1} < \dot{\varepsilon} < \tau_e^{-1}$ is chosen to be fast compared to the Rouse relaxation time, $\tau_{R,N}$, of a whole chain but slow compared to the local relaxation time of an entanglement length of unperturbed chains.

As predicted by reptation theory[5], $G(t)$ should reach a plateau value $G_N^0 = (4/5)(\rho k_B T/N_e)$ for $\tau_e < t < \tau_d$. It is indeed seen for slightly deformed polymer melts of chain size $N = 2000$ in the linear viscoelastic regime for $t > \tau_e$. Moreover, the entanglement length N_e extracted from the plateau value of $G(t)$ perfectly agrees with the estimate from a primitive path analysis (PPA). We have also checked that PPA can be extended to analyse entanglement effects in the non-linear viscoelastic regime (see the forthcoming paper[40]). The decreasing of $G(t)$ for $N = 2000$ and for $t < \tau_e$ with decreasing strain rate $\dot{\varepsilon}$ gives an indication that a characteristic strain softening sets in. In the non-linear viscoelastic regimes, the decay of $G(t)$ for $t > \tau_e$ strongly depends on the chain size N. The data for strong, but very fast elongation of the polymer melt shown by the green curve seems to interpolate the above mentioned two sets of data. At short times the normalised modulus is almost the same as for the linear case of the same strain rate. For longer times this curve interpolates between the small, but fast deformation regime and the large, but slow deformation regime. This indicates that for short times and fast deformation effects on the local packing are rather similar and independent of total strain but only dependent on strain rate, while for longer times the global conformational response dominates.

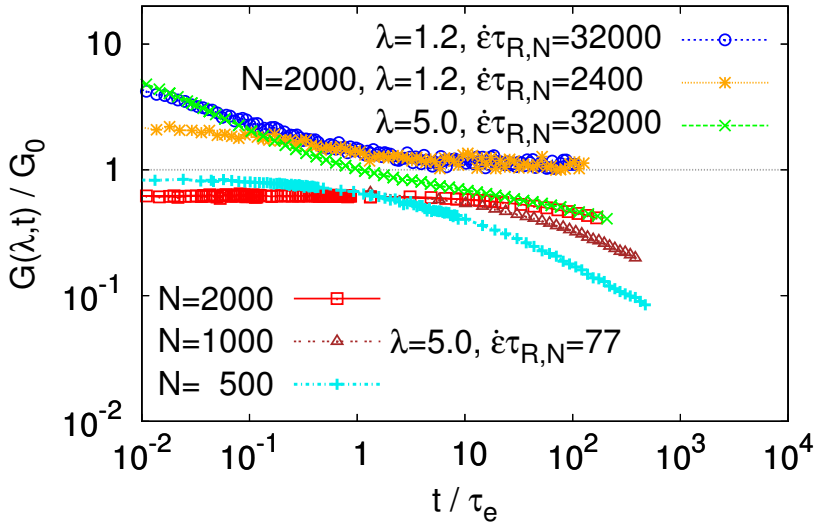

Figure 5. Rescaled stress relaxation modulus $G(\lambda, t)/G_N^0$ plotted as a function of the rescaled relaxation time t/τ_e after uniaxial elongation for $\lambda = 1.2$ and 5.0. Two different strain rates of both cases are shown, as indicated[40].

Acknowledgements

The computing time granted by the John von Neumann Institute for Computing (NIC) on JURECA at Jülich Supercomputing Centre (JSC) is gratefully acknowledged. This work has been supported by European Research Council under the European Union's Seventh Framework Programme (FP7/2007-2013)/ERC Grant Agreement No. 340906-MOLPROCOMP.

References

1. K. Kremer, *Simulation studies of soft matter: generic statistical properties and chemical details*, Eur. Phys. J B **64**, 525, 2008.
2. J. T. Padding and W. J. Briels, *Systematic coarse-graining of the dynamics of entangled polymer melts: the road from chemistry to rheology*, J. Phys-Condens. Mat. **23**, 233101, 2011.
3. K. Kremer and F. Müller-Plathe, *Multiscale simulation in polymer science*, Mol. Simulat. **28**, 729, 2002.
4. C. Peter and K. Kremer, *Multiscale simulation of soft matter systems*, Faraday Discuss. **144**, 9, 2010.
5. M. Doi and S. F. Edwards, *The theory of polymer dynamics*, Oxford University Press, New York, 1986.

6. S. F. Edwards, *The statistical mechanics of polymerized material*, Proc. Phys. Soc. London **92**, 9, 1967.
7. P. G. de Gennes, *Reptation of a polymer chain in presence of fixed obstacles*, J. Chem. Phys. **55**, 572, 1971.
8. R. S. Grahm, A. E. Likhtman, T. C. B. McLeish, and S. T. Milner, *Microscopic theory of linear, entangled polymer chains under rapid deformation including chain stretch and convective constraint release*, J. Rheol. **47**, 1171, 2003.
9. A. E. Likhtman and T. C. B. McLeish, *Quantitative theory for linear dynamics of linear entangled polymers*, Macromolecules **35**, 6332, 2002.
10. M. Doi, *Explanation for the 3.4-power law for viscosity of polymeric liquids on the basis of the tube model*, J. Polym. Sci. **21**, 667, 1983.
11. J. Klein, *The onset of entangled behavior in semidilute and concentrated polymer solutions*, Macromolecules **11**, 852, 1978.
12. M. Daoud and P. G. de Gennes, *Some remarks on the dynamics of polymer melts*, J. Polym. Sci. **17**, 1971, 1979.
13. T. C. B. McLeish, *Tube theory of entangled polymer dynamics*, Adv. Phys. **51**, 1379, 2002.
14. J. Bent *et al.*, *Neutron-mapping polymer flow: scattering, flow visualization, and molecular theory*, Science **301**, 1691, 2003.
15. L. A. Archer, *Separability criteria for entangled polymer liquids*, J. Rheol. **43**, 1555, 1999.
16. S.-Q. Wang *et al.*, *New experiments for improved theoretical description of nonlinear rheology of entangled polymers*, Macromolecules **46**, 3147, 2013.
17. R. S. Graham, E. P. Henry, P. D. Olmsted, *Comment on "New experiments for improved theoretical description of nonlinear rheology of entangled polymers"*, Macromolecules **46**, 9849, 2013.
18. Z. Wang *et al.*, *Fingerprinting molecular relaxation in deformed polymers*, Phys. Rev. X **7**, 031003, 2017.
19. K. Kremer and G. Grest, *Dynamics of entangled linear polymer melts: a molecular dynamics simulation*, J. Chem. Phys. **92**, 5057, 1990.
20. L. A. Moreira, G. Zhang, F. Müller, T. Stuehn, and K. Kremer, *Direct equilibration and characterization of polymer melts for computer simulations*, Macromol. Theory Simul. **24**, 419, 2015.
21. G. Zhang, L. A. Moreira, T. Stuehn, K. Ch. Daoulas, and K. Kremer, *Equilibration of high molecular weight polymer melts: a hierarchical strategy*, ACS Macro Lett. **3**, 198, 2014.
22. G. Zhang, T. Stuehn, K. Ch. Daoulas, and K. Kremer, *One size fits all: equilibrating chemically different polymer liquids through universal long-wavelength description*, J. Chem. Phys. **142**, 221102, 2015.
23. V. A. Harmandaris, D. Reith, N. F. A. van der Vegt, and K. Kremer, *Comparison between coarse-graining models for polymer systems: two mapping schemes for polystyrene*, Macromol. Chem. Phys. **208**, 2109, 2007.
24. V. A. Harmandaris and K. Kremer, *Predicting polymer dynamics at multiple length and time scales*, Soft Matter **5**, 3920, 2009.
25. T. Vettorel, G. Besold, and K. Kremer, *Fluctuating soft-sphere approach to coarse-graining of polymer models*, Soft Matter **6**, 2282, 2010.

26. G. Zhang, K. Ch. Daoulas, and K. Kremer, *A new coarse grained particle-to-mesh scheme for modeling soft matter*, Macromol. Chem. Phys. **214**, 214, 2013.
27. R. Auhl, R. Everaers, G. S. Grest, K. Kremer, and S. J. Plimpton, *Equilibration of long chain polymer melts in computer simulations*, J. Chem. Phys. **119**, 12718, 2003.
28. W. Tschöp, K. Kremer, J. Batoulis, T. Bürger, and O. Hahn, *Simulation of polymer melts. I. Coarse-graining procedure for polycarbonates*, Acta Polym. **49**, 61, 1998.
29. J. D. Halverson, T. Brandes, O. Lenz, A. Arnold, S. Bevc, V. Starchenko, K. Kremer, T. Stuehn, and D. Reith, *ESPResSo++: A modern multiscale simulation package for soft matter systems*, Comput. Phys. Commun. **184**, 1129, 2013.
30. G. Zhang, A. Xazirakis, T. Stuehn, V. A. Harmandaris, K. Ch. Daoulas, and K. Kremer, *Hierarchical modeling of polystyrene melts: from soft blobs to atomistic resolution*, in preparation.
31. K. Kremer and G. S. Grest, *Simulations for structural and dynamic properties of dense polymer systems*, J. Chem. Soc. Faraday Trans **88**, 1707, 1992.
32. H.-P. Hsu and K. Kremer, *Static and dynamic properties of large polymer melts in equilibrium*, J. Chem. Phys. **144**, 154907, 2016.
33. R. Everaers, S. K. Sukumaran, G. S. Grest, C. Svaneborg, A. Sivasubramanian, and K. Kremer, *Rheology and microscopic topology of entangled polymeric liquids*, Science **303**, 823, 2004.
34. S. K. Sukumaran, G. S. Grest, K. Kremer, and R. Everaers, *Identifying the primitive path mesh in entangled polymer liquids*, J. Polym. Sci. B **43**, 917, 2005.
35. P. G. de Gennes, *Scaling oncepts in polymer physics*, Cornell University Press, Itharca, New York, 1979.
36. M. Rubinstein and R. H. Colby, *Polymer Physics*, Oxford University Press, Oxford, 2003.
37. M. Pütz, K. Kremer, and G. S. Grest, *What is the entanglement length in a polymer melt?*, Europhys. Lett. **49**, 735, 2000.
38. K. Kremer and K. Binder, *Dynamics of polymer chains confined into tubes: Scaling theory and Monte Carlo simulations*, J. Chem. Phys. **81**, 6381, 1984.
39. H.-P. Hsu and K. Kremer, *Detailed analysis of Rouse mode and dynamic scattering function of highly entangled polymer melts in equilibrium*, Eur. Phys. Special Topics **226**, 693, 2017.
40. H.-P. Hsu and K. Kremer, *Primitive path analysis and stress distribution in highly strained macromolecules*, ACS Macro Lett. **7**, 107, 2018.